Reprinted from SPIE Vol. 210—2nd European Congress on Optics Applied to Metrology © 1980 by the Society of Photo-Optical Instrumentation Engineers, Box 10, Bellingham, WA 98225 USA

Compact device for interferometric holography

Lia M. Zerbino, Héctor J. Rabal, Mario Garavaglia
Centro de Investigaciones Opticas. (CONICET-UNLP-LEMIT)
Camino Parque Centenario e/505 y 508-Gonnet. Casilla de Correo 124
1900La Plata, Argentina

Abstract

The diffraction phenomenon produced by a Fabry-Perot interference pattern record is analized. As a result of this analysis, a compact device for interferometric holography has been developed. It is presented as example an application of this device to the interferometric determination of deformations in a loaded metallic cantilever.

I. Introduction

In a previous report[1] it was analyzed the geometry and profiles of the interference diagrams produced by multiple reflections when a light beam passes through a plane wedge with highly reflective surfaces, as in the case of a misaligned Fabry-Perot interferometer. The analytical treatment follows those by Brossel[2], Born and Wolf[3], and Aebischer[4], but taking into account the refractive index of the transparent media, and the possibility that the monochromatic point source and the observation plane could be located near the interferometer.

The geometry and profiles of the moiré patterns obtained by superposition of the interference diagram records, were also calculated. Both the interference diagram records and the moiré patterns show interesting diffraction behaviour.

In this paper we detail the diffraction phenomenon produced when a light beam impinges on a pupil $P(y_1,z_1)$ containing a photographic record of a Fabry-Perot interference diagram, or a moiré pattern of these diagrams.

Following the Gaussian scalar diffraction theory, the field distributions are obtained as solutions of Maxwell equations with specified pupil boundary conditions. Then, the system is linear, and it is possible to express the response function of the system $g_2(y_2,z_2)$ to an arbitrary input $g_1(y_1,z_1)$, in terms of the Green's function of the system. When the optical system is space-invariant, we are able to write

$$g_2(y_2,z_2) = g_1(y_1,z_1) * H \tag{1}$$

where $*$ indicates the convolution product, and H is the Green's function of the system. Under the Rayleigh-Sommerfeld[5] scalar formulation, H takes the form

$$H(P_2,P_1) = \frac{\exp[i\frac{2\pi}{\lambda}|\overline{r_{21}}|]}{i\lambda\,|\overline{r_{21}}|}\cos(\bar{n},\overline{r_{21}}) \tag{2}$$

where H is the impulse response at $P_2(y_2,z_2)$ to a ray coming from a light point source located at $P_1(y_1,z_1)$ on the pupil. $\overline{r_{21}}$ is the vector pointing from P_2 to P_1, and $\bar{n}$ is the normal to the pupil, as shown in Figure 1.

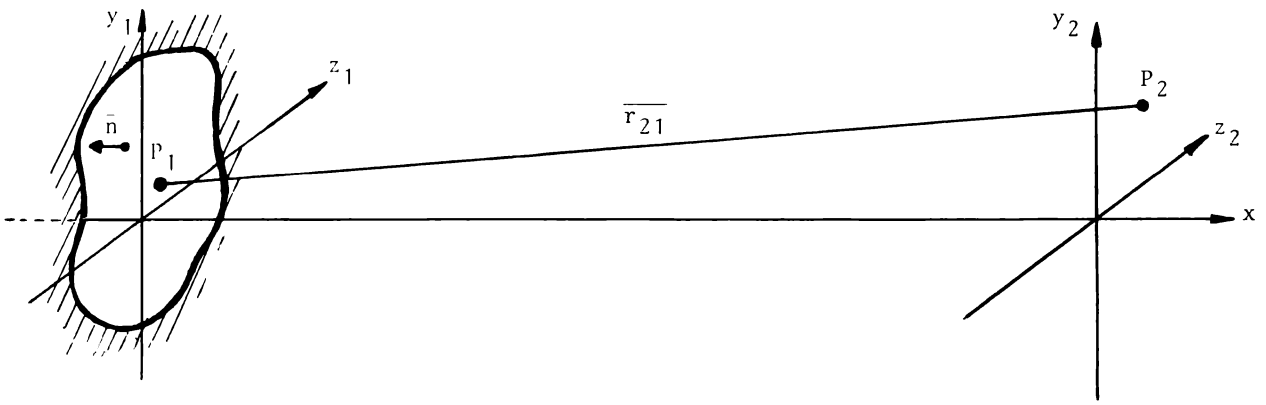

Figure 1

When the plane y_2z_2 is sufficiently far from the plane y_1z_1, Fresnel approximations for paraxial rays are valid, then:

$$H = \frac{\exp[i\frac{2\pi}{\lambda} x]}{i \lambda x} \exp\left(\frac{i\pi}{\lambda x}[(y_2-y_1)^2 + (z_2-z_1)^2]\right) \quad (3)$$

If we suppose that $g_1(y_1,z_1) = 0$ outside the pupil P, it is possible to write equation (1) as:

$$g_2(y_2,z_2) = \frac{\exp[i\frac{2\pi}{\lambda} x]}{i \lambda x} \iint_{-\infty}^{\infty} g_1(y_1,z_1) \exp\{\frac{i\pi}{\lambda x}[(y_2-y_1)^2+(z_2-z_1)^2]\} dy_1 dz_1 \quad (4)$$

We will use this equation to calculate the field distribution $g_2(y_2,z_2)$ where $g_1(y_1,z_1)$ represents a wave transmitted by a pupil whose transmittance is that of a Fabry-Perot interference diagram photographic record.

Section II will analyze the field distribution $U(y_2,z_2)$ produced by the wave diffraction in the pupil. Calculations of the image positions and magnifications by the recorded interference Fabry-Perot patterns, which are like those obtained by Fresnel zone plates, are included in Section III. Section IV briefly extends the previous analysis to the case of moiré superposition of various interference patterns. Section V is devoted to the theoretical formulation and experimental development of a compact holographic device based on the behaviour of the images obtained by multiple reflections.

II. Diffraction through interference pattern records

Let S_0 be a monochromatic light point source of wavelength λ_0 located at $P_0(x_0,y_0,z_0)$, T a transparency located at plane $x = x_1$, and $P_2(x_2,y_2,z_2)$ the observation point, as it is shown in Figure 2. T consists of a record of interference patterns obtained with a Fabry-Perot interferometer limited by a pupil P

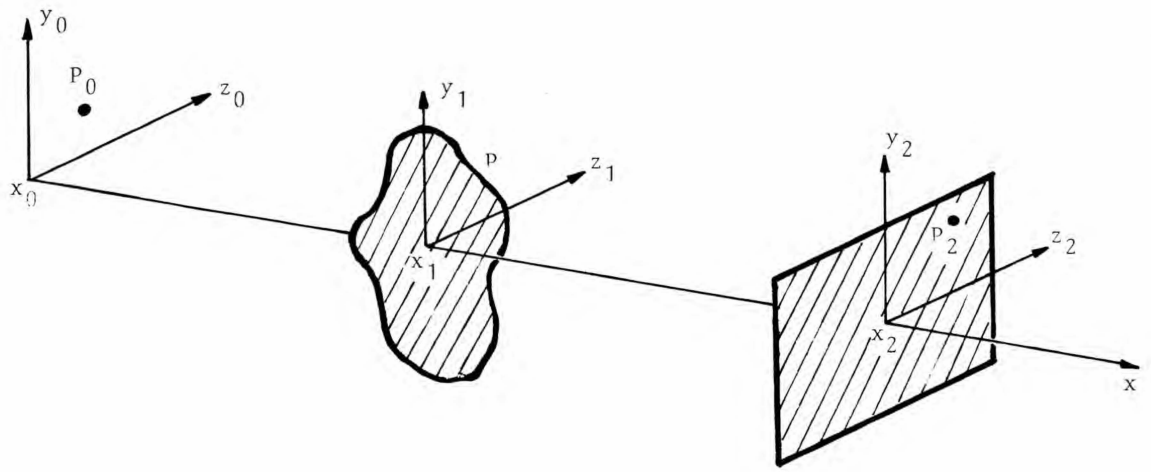

Figure 2

The spherical wave of amplitude A_0 originated at P_0 produces on the pupil an incident field

$$A_0 \frac{e^{ik_0r_{10}}}{r_{10}} \qquad \text{, where } k_0 = \frac{2\pi}{\lambda_0}$$

Let $P(y_1,z_1)$ be the function describing the pupil P and $t(y_1,z_1)$ its amplitude transmittance function; then the value $U(y_1,z_1)$ of the transmitted field immediately behind the interferometer is

$$g_1(y_1,z_1) = A_0 \frac{e^{ik_0r_{10}}}{r_{10}} P(y_1,z_1)\, t(y_1,z_1) \quad (5)$$

By introducing this expression into equation (4) and rearranging terms, the field $U(y_2,z_2)$ at P_2 results

$$U(y_2,z_2) = Q \iint_{-\infty}^{\infty} P(y_1,z_1)\ t(y_1,z_1)\ \exp i\Phi(y_1,z_1)\ \exp i\Psi(y_1,z_1)\ dy_1\ dz_1 \qquad (6)$$

where

$$Q = \frac{e^{ik_0(x_1-x_0)}}{i\lambda_0 (x_1-x_0)} \frac{e^{ik_0(x_2-x_1)}}{(x_2-x_1)} \exp\left[\frac{ik_0}{2}\left(\frac{y_0^2+z_0^2}{x_1-x_0} + \frac{y_2^2+z_2^2}{x_2-x_1}\right)\right] A_0 \ ,$$

$$\Phi = k_0 \frac{y_1^2+z_1^2-2(y_0y_1+z_0z_1)}{2(x_1-x_0)} \qquad \text{and} \qquad \Psi = k_0 \frac{y_1^2+z_1^2-2(y_2y_1+z_2z_1)}{2(x_2-x_1)}$$

The transmittance $t(y_1,z_1)$ of a developed photographic record takes, in general, the form

$$t(y_1,z_1) = t_0 + \beta I_t \qquad (7)$$

where t_0 is a uniform transmittance which depends on the incident wave intensity; β is a factor related with the characteristics of the recording media and the developing process; and I_t is the intensity distribution transmitted through the interferometer when the interference pattern was recorded.

As it was demonstrated in Reference [1],

$$I_t = (t_1t_2)^2 \sum_{q,m=0}^{p} (r_1r_2)^{m+q} \exp[ik(\delta_q-\delta_m)]\left(1-\frac{\delta_q}{r_q}\right)\left(1-\frac{\delta_m}{r_m}\right) I_i \qquad (8)$$

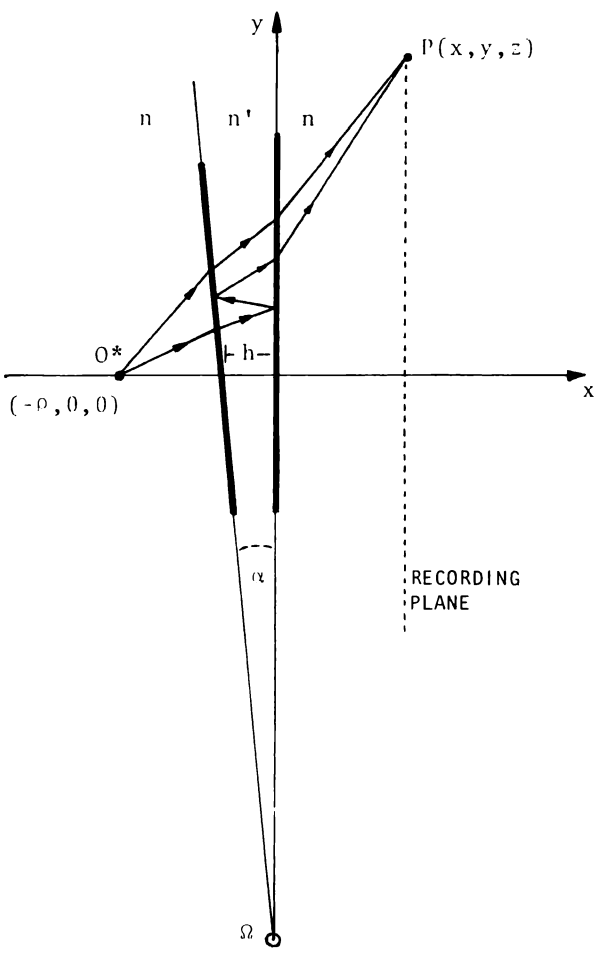

Figure 3

where t_1, t_2, r_1, r_2 are the transmission and reflection coefficients of the two interferometer surfaces; $k = 2\pi/\lambda$, with λ as the wavelength of the ligth whose intensity I_i was used in the recording process; δ_q and δ_m are the optical path differences of rays reflected q or m times on the interferometer surfaces; and r_q and r_m are the respective optical paths of those rays up to recording plane.

To introduce in equation (6) the value of $t(y_1,z_1)$ given by equation (7), we must write δ_q, δ_m, r_q and r_m in equation (8) as functions of x_1, y_1, z_1 coordinates. Such expressions of δ_i and r_i, in the most general case, were calculated in Reference [1].

In the particular case of a misaligned air spaced Fabry-Perot interferometer ($n = n'$), we obtein the following expression for δ_q:

$$\delta_q = 2qhn\left(1-\frac{y^2+z^2}{2(x+\rho)^2}\right) + 2q\alpha\rho n \frac{y}{x+\rho} \qquad (9)$$

where h is the mean separation between plates;
α is the misalignment angle;
$(-\rho,0,0)$ are the coordinates of the source O*;
and x are the distance from the interferometer to the recording plane, as shown in Figure 3.

The developed plate is located at the

the pupil plane $y_1 z_1$, as shown in Figure 2. Then, the transmittance $t(y_1,z_1)$ will be given by

$$t(y_1,z_1) = t_0 + \beta I_i (t_1 t_2)^2 \sum_{q,m=0}^{p} \Delta (r_1 r_2)^{m+q} \exp\{ik2n(q-m)[h - h\frac{y_1^2+z_1^2}{2(x'+\rho)^2} + \frac{\alpha\rho y_1}{x'+\rho}]\} \qquad (10)$$

where x' was the distance from the interferometer to the photographic material at the recording time. For the sake of brevity we have called

$$= (1 - \frac{\delta_q}{r_q})(1 - \frac{\delta_m}{r_m})$$

It is possible to transform the double summa in equation (10), obtaining:

$$t(y_1,z_1) = t_0 + \beta I_i T^2 \frac{R^{p+1}}{R^2-1} \{(R^{p+1} - R^{-(p+1)}) + \sum_{s=1}^{p} \Delta (R^{p-s+1} - R^{-p+s-1})(e^{isk\delta} + e^{-isk\delta})\} \qquad (11)$$

where $R = r_1 r_2$; $T = t_1 t_2$; and

$$\delta = 2n (h - h \frac{y_1^2 + z_1^2}{2(x'+\rho)^2} + \frac{\alpha\rho y_1}{x'+\rho})$$

Then, the field at $x = x_2$ is equal to:

$$U(y_2,z_2) = Q \{t_0 + \beta I_i \frac{T^2 R^{p+1}}{R^2-1} (R^{p+1} - R^{-(p+1)}) L_1 +$$

$$+ \beta I_i \frac{T^2 R^{p+1}}{R^2-1} \sum_{s=1}^{p} \Delta (R^{p-s+1} - R^{-p+s-1}) (e^{ik2nsh} L_{2_s} + e^{-ik2nhs} L_{2_{-s}})\} \qquad (12)$$

where

$$L_1 = \iint_{-\infty}^{\infty} P(y_1,z_1) \exp\{i(A_1 y_1^2 + B_1 y_1)\} \exp\{i(A_1 z_1^2 + B_1' z_1)\} dy_1 dz_1 \qquad (13)$$

with

$$A_1 = \frac{k_0}{2} (\frac{1}{x_1 - x_0} + \frac{1}{x_2 - x_1}) \quad ,$$

$$B_1 = -k_0 (\frac{y_o}{x_1 - x_0} + \frac{y_2}{x_2 - x_1}) \qquad \text{and} \quad B_1' = -k_0 (\frac{z_0}{x_1 - x_0} + \frac{z_2}{x_2 - x_1})$$

and

$$L_{2_s} = \iint_{-\infty}^{\infty} P(y_1,z_1) \exp\{i(A_{2_s} y_1^2 + B_{2_s} y_1)\} \exp\{i(A_{2_s} z_1^2 + B_2' z_1)\} dy_1 dz_1 \qquad (14)$$

with

$$A_{2_s} = A_1 - \frac{knsh}{(x'+\rho)^2} \quad , \quad B_{2_s} = B_1 + \frac{k2ns\alpha\rho}{x'+\rho} \quad \text{and} \quad B_2' = B_1'$$

To each s value, equation (14) gives one expression of the integrals L_{2_s} and $L_{2_{-s}}$, and it is possible to choose the plane x_2 in such a way that A_{2_s} be equal to zero. Then, on that plane, L_{2_s} will be the Fourier transform of the $P(y_1,z_1)$ aperture function. In fact, if $A_{2_s} = 0$, L_{2_s} will be:

$$L_{2_s} = \iint_{-\infty}^{\infty} P(y_1,z_1) \exp(iB_{2_s} y_1) \exp(iB_2' z_1) dy_1 dz_1 \qquad (15)$$

This condition implies that:

$$A_{2_s} = \frac{k_0}{2}\left(\frac{1}{x_1-x_0} + \frac{1}{x_2-x_1}\right) - \frac{knsh}{(x'+\rho)^2} = 0 \qquad (16)$$

and this is the lens makers' formula for a lens with focal length

$$F = \frac{k_0(x'+\rho)^2}{2nsh} \quad ,$$

located at the plane $x = X_1$. The quantities (x_1-x_0) and (x_2-x_1) are the object and image distances, respectively.

Then, each term in L_{2_s} contributes to the field, giving the Fourier transform of the aperture in a plane $x = x_2$, where $A_{2_s} = 0$.

This analysis is also true for terms in $L_{2_{-s}}$. In fact, $A_{2_{-s}} = 0$ at the planes $x = x_2'$, which are symmetric with respect to the developed plate, to those planes $x = x_2$ where $A_{2_s} = 0$ for the same values of $|s|$.

We must note that A_1 vanishes if and only if $x_2 = x_0$, so L_1 in equation (13) represents a divergent wave from x_0 . When the dimension of the pupil $P(y_1,z_1)$ is very large, this wave will be transmitted without perturbation.

Then, the diffraction phenomena observed in a Fabry-Perot interference ring pattern can be interpreted as being produced by lenses with focal lengths

$$F = \pm \frac{k_0(x'+\rho)^2}{k2nsh}$$

III. Position and magnification of images

From the condition $A_{2_s} = 0$ it is possible to find out the possitions of focal planes. Besides, the other two coordinates of the focus are obtained from making zero the coefficients B_{2_s} and B_2' in equation (14).

In such a way, we can calculate:

$$y_{2_s} = \left(\frac{2ns\alpha\rho}{x'+\rho}\frac{\lambda_0}{\lambda} - \frac{y_0}{x_1-x_0}\right)(x_2-x_1) \quad , \text{ and } \quad z_{2_s} = -z_0\frac{x_2-x_1}{x_1-x_0}$$

Variations $(\Delta y_0, \Delta z_0)$ in the light source coordinates will give as a result, variations in the image coordinates, in the following way:

$$\Delta y_i = -\frac{x_2-x_1}{x_1-x_0}\Delta y_0 \quad , \text{ and } \quad \Delta z_i = -\frac{x_2-x_1}{x_1-x_0}\Delta z_0$$

Thus, the Fabry-Perot ring pattern behaves like a lens whose magnification is

$$M = \frac{x_2-x_1}{x_1-x_0}$$

as geometrical optics predicts for an ideal lens.

These results reminds us those ones obtained with Fresnel zone plates. Then, we have found out that the diffraction by Fabry-Perot rings gives rise to the formation of multiple images of the light source.

IV. Diffraction by moirés

If a ring pattern D_1 diffracts the light emitted from a light point source S_0 and focus it on an image of such a source, it is reasonable to expect, according with the superposition principle, that in the moiré of two or more of such D_n patterns, each one will contribute to the field distribution, given rise to point images of the source s . These point images are located at positions calculated in accordance with equation of Section III.

For example, in the case of the moiré of two slightly displaced equal patterns, each one of them gives rise to the formation of an image of the source which lies at same distance from the plate. Then it is easy to see that these points act as the secondary source in a Young's experiment. Those secondary sources will produce an interference phenomenon without localized fringes.

On the other hand, the record of the displaced rings could be interpreted as produced by recording the Fabry-Perot interference rings of light coming from two point sources located at the same distance from the interferometer. From this point of view, each pair of imaged points generated by using the moiré record as a diffracting aperture, could be interpreted as the holographic images of the two original point light sources.

V. Holography using a Fabry-Perot interferometer

Let suppose we make an experiment with a device similar to that shown in Figure 4. The

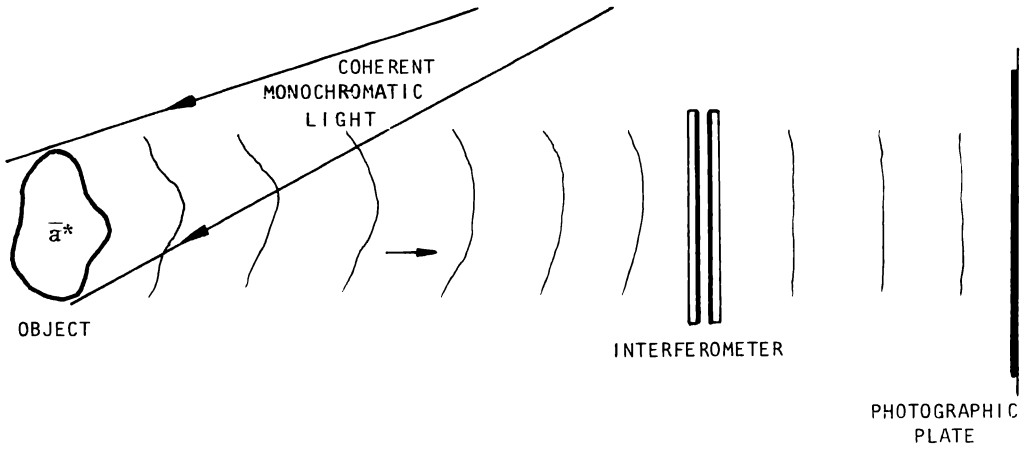

Figure 4

object is illuminated with coherent and monochromatic light. The light scattered by the object, $\bar{a}^*$, impinges on a photographic plate passing through a Fabry-Perot interferometer.

The effect produced by the interferometer is similar to the simultaneous existence of p+1 homothetic objects whose amplitudes are proportional to each other, and whose phases differs from each other in

$$\frac{2\pi}{\lambda}\,\delta$$

where δ is the optical path difference.

If $\bar{a}_n$ is the amplitude of the incident field on the plate, corresponding to the $n^{\underline{th}}$ image of the original object, the total field on the plate will be

$$\sum_{n=0}^{p} \bar{a}_n$$

and the recorded intensity I is expressed as:

$$I = \sum_{n=0}^{p} |\bar{a}_n|^2 + \sum_{\substack{n,i=0 \\ n \neq i}}^{p} \bar{a}_n\, \bar{a}_i^*$$

Working in the linear region of the photographic plate, the transmittance of the developed record will be $t = t_0 + \beta I$.

If in the reconstructing process we illuminate the record with a field $\bar{B}$, the output light field will be

$$U_2 = \bar{B}t$$

Supposing that the reconstructing wave has the same amplitude and phase than those generated in one of the objects, for example $\bar{B} = \bar{a}_j$, the field equation takes the form:

$$U_2 = \bar{a}_j \left(t_o + \beta \sum_{n=0}^{p} |\bar{a}_n|^2\right) + \beta\, \bar{a}_j \sum_{\substack{n,i=0 \\ n \neq i}}^{p} \bar{a}_n\, \bar{a}_i^* + \beta \sum_{n=0}^{p} \bar{a}_n\, |\bar{a}_j|^2$$

We see that the first term is proportional to the incident field, and the second one corresponds to the interference between different orders. The third term reconstructs a field proportional to that generated from every $\bar{a}_n$ homothetic object. Besides, the reconstruction efficiency will increase as the reconstructing wave becomes more similar to some object wave $\bar{a}_n$. Then, it follows a straightforward possibility of doing holographic interferometry in a real time mode.

The diffraction efficiency of the holograms obtained with this new method is not so high as in conventional holography. However, as it does not need an explicit reference beam to construct the hologram, it offers the advantage of making a compact holographic camera. With it, holograms of moderate quality can be made outside the experimental laboratory conditions.

Figure 5 shows the experimental scheme of the compact holographic camera for taking holograms of objects illuminated with coherent and monochromatic light.

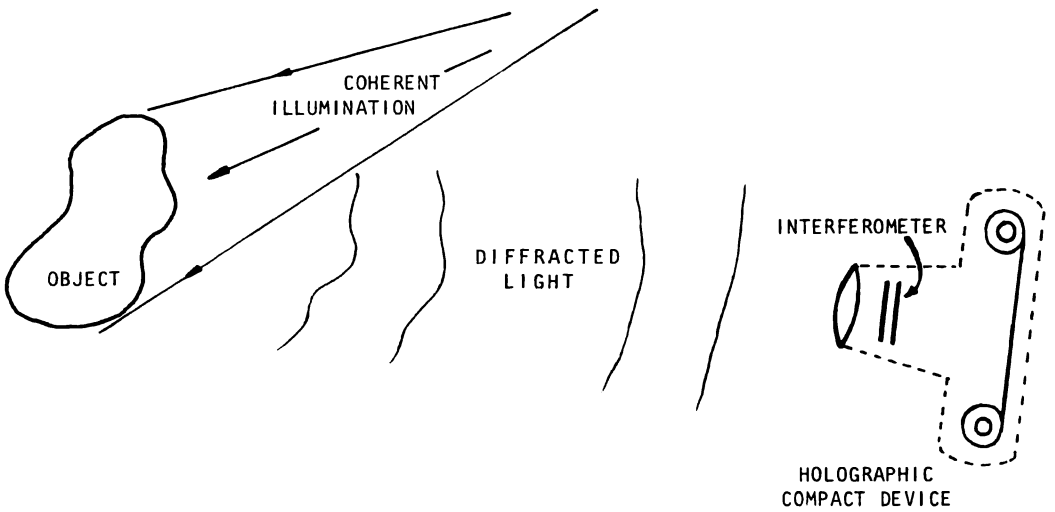

Figure 5

By changing the focus of the camera objective, it is possible to record image holograms of reasonable efficiency.

The interferometer can be solid, glassmade, with both faces semispecular plated. It is also desirable to introduce a slight misalignment between faces, which will produce the effect of an off-axis hologram.

We obtained "image" holograms locating a 1 cm thick glass interferometer inside a 35 mm conventional photographic camera. We used Kodak SO 253 holographic film of fast response, and Kodak 649F with slow response, and the objects were illuminated, indistinctly, with a 2 W argon laser or a 1 mW He-Ne laser.

We made interferential holograms of a cantilever measuring 12 cm long, 2,1 wide and 0,4 width fixed in one extreme and loaded in the other with 20 g weights.

The photographs of Figures 6 and 7 show the experimental set-up and the reconstructed real and virtual images.

We must note that, as the recorded interference pattern is obtained by multiple reflection of the light inside the interferometer, it is possible to consider the case in which the light is spacially incoherent. In this case the interference occurs only between rays coming from corresponding points of consecutive images.

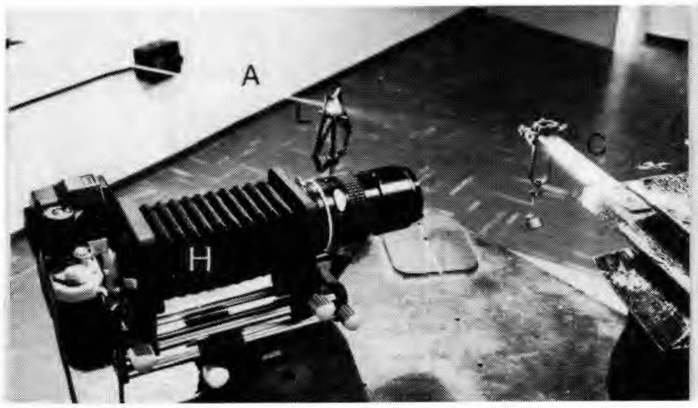

Figure 6. Experimental setup.(A)Argon laser beam,(L)lens,(H)holographic compact device,(C)cantilever loaded.

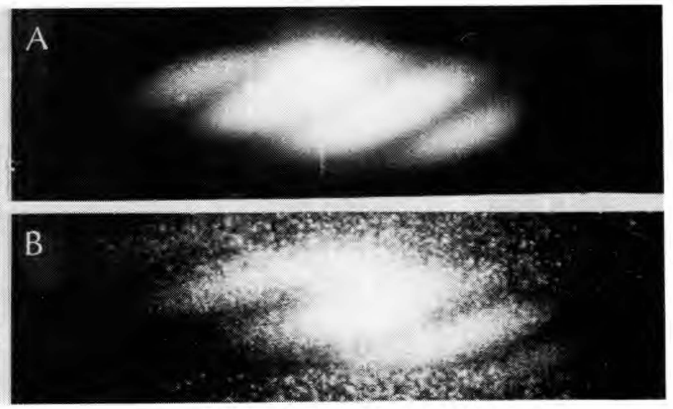

Figure 7. Reconstructed images.
(A) virtual
(B) real

VI. Acknowledgments

The invaluable support provided by the Secretaría de Estado de Ciencia y Tecnología, Argentina, the Comisión de Investigaciones Científicas de la Provincia de Buenos Aires, Argentina, and the Organization of American States is gratefully acknowledged.

VII. References

1. -Zerbino, L. M. and Garavaglia, M., Intensity distribution in multiple reflection interference patterns. Part I, Reunión Nacional de Física, Villa Giardino, Argentina, October 30-November 2, 1979.
-Rodríguez, N., Torroba, R., Zerbino, L. M. and Garavaglia, M., Part II, Reunión Nacional de Física, Villa Giardino, Argentina, October 30-November 2, 1979.
2. Brossel, J., "Multiple-beam localized fringes: Part I - Intensity distribution and localization", Proc. Phys. Soc., London, Vol. 59, pp. 224-234, March, 1947.
3. Born, M. and Wolf, E., Principles of Optics, Pergamon Press, London, 1959.
4. Aebischer, N., "Calculs de profils dissymétriques observables sur des figures d'interférences en ondes multiples sphériques", Nouv. Rev. d'Optique Appliquée, Vol. 2, N°6, pp. 351-366, 1971.
5. Goddman, J. W., Introduction to Fourier Optics, McGraw-Hill, New York, 1968.